Development of a Stress-Strain Path Controlled Triaxial Apparatus to Understand the Behaviour of Silty Sand

A. T. M. Z. Rabbi[1 and 2], M. M. Rahman[1 and 3], K. Mills[1], and D. A. Cameron[1]
[1]*UniSA STEM, University of South Australia, Mawson Lakes, Australia*
[2]*CMW Geosciences, Mitsubishi Admin Building, 1 Tonsley Boulevard, Tonsley, Australia*
[3]*ScaRCE - Smart Infrastructure and Built Environments Research Center, University of South Australia, Mawson Lakes, Australia*
E-mail: zillur.rabbi@mymail.unisa.edu.au

ABSTRACT: Triaxial tests are widely used to determine the shear strength, material properties and instability behaviour of soil. The conventional isotropically consolidated drained and undrained triaxial compression tests under constant confining stresses, fail to simulate many field stress conditions such as K_0-consolidation for zero radial strain or the reduction of lateral confinement at constant shear stress and associated instability behaviour of slopes. Such strain or stress path controlled tests need special arrangements and control systems. In this paper, a newly developed triaxial apparatus, capable of stress-strain path controlled test, is described. The main feature of this apparatus is the precise measurement and control system, which permits individual control of the cell pressure, pore water pressure, vertical stress and axial strain. The apparatus was used to study the stress-strain behaviour of a South Australian silty sand under different stress-path testing such as isotropic and K_0-consolidated undrained and drained shear, constant shear drained (CSD) and constant mean stress (CMS) tests. Critical state conditions were achieved with uniform soil deformation at large axial strains, except in the case of the constant shear drained (CSD) tests where a gradual reduction of lateral confinement accelerated sample failure.

KEYWORDS: Stress-path, Triaxial apparatus, Critical state, Constant shear drained, Constant mean stress.

1. INTRODUCTION

For the development of critical state soil mechanics (CSSM) (Roscoe et al., 1958), it is important to have a reliable determination of critical state of soil in which ongoing plastic strain is occurred at constant stress and constant volume (Schofield and Worth, 1968). Critical state of a sandy soil can be obtained in laboratory triaxial tests on representative soil samples, however, challenges exists with available devices in fulfilling conditions such as obtaining large displacement, sample homogeneity and stress-strain distribution at large strain, constant volume or pore water pressure development etc. Appropriate testing and sample preparation methodologies and accurate measurement and control system are necessary to achieve critical state. Attempts to overcome such challenges over the years (Bobei et al., 2009; Lo et al., 1989; Omar and Sadrekarimi, 2014; Rahman and Lo, 2014) have been performed mainly under conventional undrained and drained stress paths, sheared at constant confining stress, σ_3 (Cubrinovski and Ishihara, 1998; Ishihara, 1993; Murthy et al., 2007; Rabbi et al., 2014; Rahman et al., 2008). Other researchers used stress path tests to simulate particular field stress conditions such as constant shear drained (CSD) tests (Chu et al., 2012; Rabbi et al., 2019; Sasitharan et al., 1993; Zhu and Anderson, 1998), constant mean stress (CMS) or constant p' tests (Gajo et al., 2000; Jakobsen et al., 1999; Lade and Ibsen, 1997). The typical applications of different stress-strain path testing are presented in Table 1. Although importance of stress-strain path tests is recognised, the data for these tests are rare in the literature and often revealed contradictory outcomes e.g. some researchers found unstable behaviour during CSD tests before the effective stress path reached the failure envelope while others found complete stability before reaching the failure envelope. Therefore, new and reliable stress-strain path testing are important, which is the motivation for the development of this stress-strain path controlled triaxial apparatus. The special stress or strain control-loading requirement for specific field condition and the required control systems are also discussed.

Most of the triaxial studies of sand simulated the initial field condition such as the depth of soil and confinement using isotropic consolidation and then applied deviatoric stress under drained or undrained condition to determine the stress-strain, critical state and instability behaviour (Rahman and Lo, 2012; Thevanayagam et al., 2002; Yang, 2002). However, natural ground is more likely consolidated under a K_0-condition with no lateral strain. The reason for considering an isotropic condition is its simplicity. Maintaining the K_0-condition in triaxial system is complex process, which requires an accurate measurement and control of strain/stress through feedback system that is often not available in most of the triaxial systems. Although isotropic consolidation is a common practice in triaxial testing system, some researchers have found that K_0-consolidation has significant effects on stress-strain, critical state and instability behaviour (Finno and Rechenmacher, 2003; Fourie and Tshabalala, 2005; Nguyen et al., 2016; Rabbi et al., 2018; Rabbi et al., 2019). Therefore, isotropic and K_0-consolidated triaxial tests data for same soil are required to understand the role of consolidation on mechanical behaviour of soil.

This paper discusses a newly developed stress path controlled triaxial apparatus to study the behaviour of South Australian silty sand under conventional and special stress path triaxial tests. The new triaxial system was commissioned by modifying an existing ELE load frame (Digital Tritest) accommodating 100 mm x 100 mm specimens. The apparatus has properly enlarged end platens, free ends and uniform sample preparation methods, which greatly reduce untoward boundary constraints. One of the main features of this apparatus is its precise control and measurement system, which can individually control the cell pressure, pore water pressure, vertical stress and axial strain.

Drained and undrained triaxial compression tests were conducted for silty sand after both isotropic (CID and CIU) and K_0-consolidation (K_0D and K_0U). Results from isotropically and K_0-consolidated undrained and drained tests, isotropically consolidated CSD and CMS tests are presented in this paper to illustrate the performance of the triaxial system. The data for K_0-consolidation was also compared with oedometer tests for the same material conducted for a different purpose.

2. TRIAXIAL TESTING SYSTEM

2.1 Design

The design of the computer-controlled triaxial testing system commissioned in the laboratory is schematically illustrated in Figure 1. An ELE load frame with a modified conventional triaxial cell was used. In order to obtain uniform stress distribution, enlarged end platens and free end techniques were used (Lo et al., 1989; Rowe and

Barden, 1964), which was found effective in previous studies (Bobei et al., 2009; Lo et al., 2010; Zhang et al., 2017).

The cell water and pore water are stored in acrylic water tanks pressurised through bladder type air/water interfaces to avoid re-introduction of air to the de-aired water. Electronic pneumatic regulators under computer control were used to apply cell/pore pressure through air/water interfaces. Manually operated regulators are installed to use optionally in case of mechanical failure. A GDS pressure volume controller was coupled to the pore pressure connections to measure or control pore water volume/pressure.

Table 1 Typical application of stress path triaxial tests

Tests	**Applications**
CIU K_0U	Determination of shear strength parameters, for slope stability analysis, liquefaction analysis, offshore ground engineering etc.
CID K_0D	Determination of shear strength parameters, coefficient of consolidation, permeability, parameters for constitutive modelling, for slope stability analysis, offshore ground engineering etc.
CSD	Analysis of strength parameters and liquefaction in complex loading condition such as water infiltration, ground water rising, piping of water, lateral stress relief, erosion of slope faces etc.
CMS	Analysis of strength parameters in all practical conditions where deviator stress increases with a reduction of lateral confinement such as at the toe of a cut slope.

2.2 Operation and Measurement Systems

During a test sequence, the active components of the system were under computer control. The ELE load frame (Digital Tritest 50) was driven to achieve a desired rate of displacement using commands sent via an RS232 interface. Axial load was measured by a submersible STALC3 load cell located inside the cell, just above the top platen. The capacity of the load cell was 15 kN and with an accuracy of ±0.05%. For force control, a feedback loop was used with a displacement rate projected for the next time step of the loop. This was done by estimating the small strain stiffness for the specimen to apply a displacement rate so that the applied force was lagging the target value. Given that loading rates are slow in these testing, this has proved satisfactory, and importantly it avoids overshoot problems at cusps on a loading curve. Thus, testing can be done for either strain control or stress control. A potentiometric displacement transducer (LVDT) with an accuracy of 0.002 mm was used to measure axial deformation.

Cell pressure was controlled using a pressure regulator and measured using a pressure transducer mounted just outside the cell. An Advanced Digital Pressure Volume Controller (DPVC) (GDS, 2000) with 2 MPa pressure and 1000 cubic cm volume capacity was used to apply back pressure and to monitor or control volume change of the specimen. The DPVC has an accuracy of 0.1% in both pressure and volume measurement. In an undrained test, the DPVC seeks a constant volume and measures the change in pore water pressure. In a drained test, the DPVC seeks a constant pore water pressure and allows volume change. It can switch smoothly from undrained to drained mode or vice versa during testing through computer control. The host computer controls the DPVC by sending and receiving signals through an RS232 interface.

In addition to the DPVC, a pore water pressure transducer was also fitted to monitor the pore water pressure connected to the top of platen and placed just outside the cell. This transducer provided a cross check of the pressure readings from the DPVC and the uniformity of the pore water pressure throughout the specimen.

2.3 Computer Program for Control and Data Logging

An in-house computer program was developed using LabVIEW to control and monitor fully computer controlled triaxial testing system. The software has a *central control program* segment, a *monitoring program* and a set of *test phase modules* that perform the different test phases.

The *central control program* provides for test initialization, subsequent test module selection and controlled shutdown. It also handles all raw data acquisition, and the control loop for the loading frame. The *monitoring program* derives the current values for the test state from the raw data values. It has tab-selected graphical displays, and also writes the test log file. The processed values are written back to the *central control program's* data area. *Test phase modules* for the tests can be activated one at a time by the user. The whole computer program sequence flow chart is shown in Figure 2. To date there are seven different *Test phase modules* in the program which are; Back pressure module, *B*-response module, Isotropic consolidation

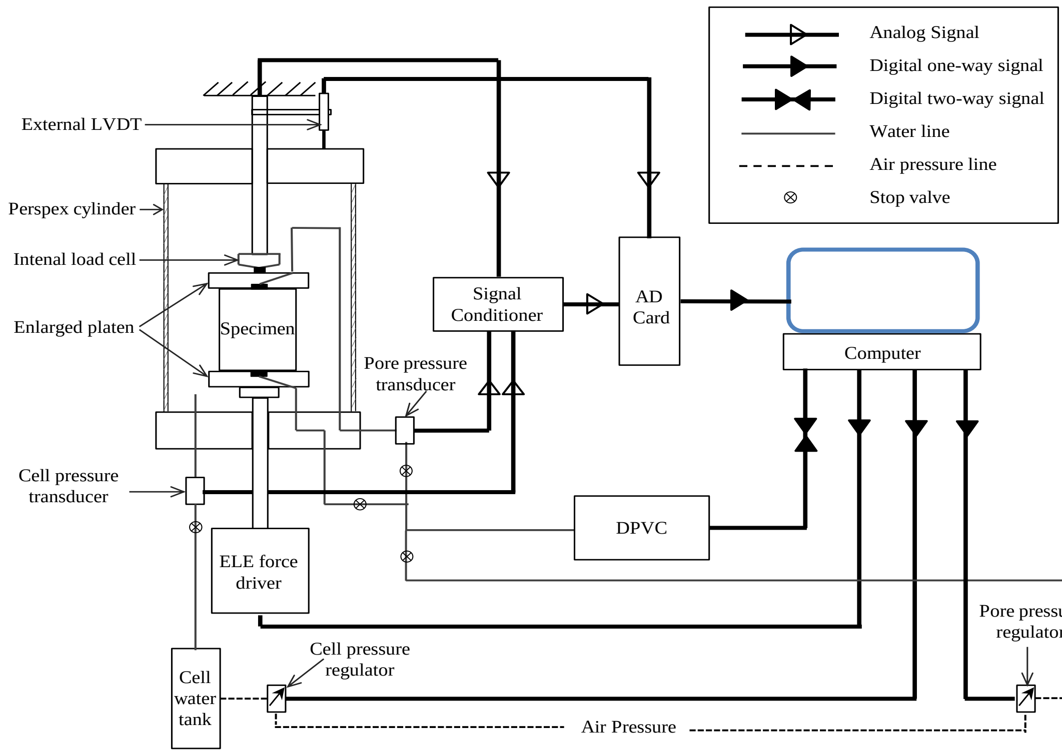

Figure 1 Line diagram of triaxial testing system

module, Drained monotonic loading module, Undrained monotonic loading module, K_0-consolidation module and "$p - q - u$ table" module. The following sub-sections briefly describe different control modules of the program.

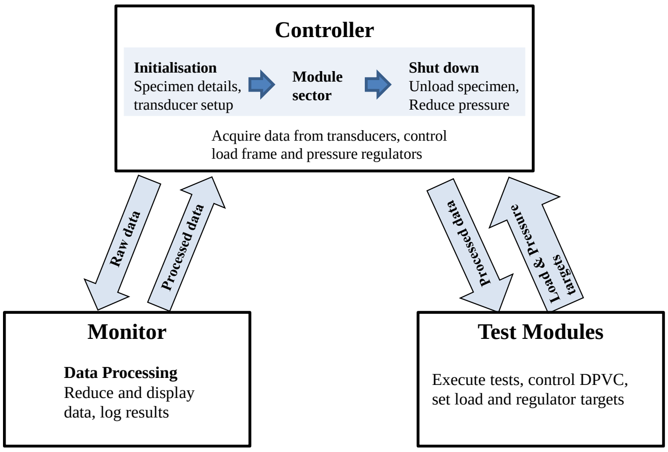

Figure 2 Control Program Architecture

2.3.1 Back Pressure Module

This module is programmed to apply back pressure saturation by increasing cell pressure, σ_3 and pore pressure, u simultaneously to the desired values in increments, keeping the effective stress of the specimen constant. The simultaneous rate of increment of cell pressure and pore pressure was small enough (2 kPa/min in this study) to allow uniform pressure distribution within the specimen. One of the specific features of this apparatus is the 'bedding control' (B) which allows the ram movement during the back pressure stage to maintain a target deviator stress (1 kPa in this study). This allows the monitoring and measurement of vertical deformation due the saturation of the soil specimen and subsequently allows tracking void ratio changes prior to consolidation and shearing.

2.3.2 B-response Module

This module is programmed to measure Skempton's pore pressure parameter, B by increasing cell pressure, σ_3 to a target value and measuring pore pressure, u, without allowing volume change in the DPVC. B-value is calculated from the change in σ_3 and u. This can be repeated for several stress increments until either a cell stress limit is reached, or the value of B is greater than a minimum level. Although, a B-value can be measured manually by closing the pore water valves and increasing σ_3, this module helps in achieving an implied degree of saturation under minimum back pressure.

2.3.3 Isotropic Consolidation, Undrained and Drained Monotonic Loading Module

Isotropic consolidation module commands the cell pressure regulator to increase cell pressure, σ_3 to the target cell pressure at a constant rate while the DPVC measured the volume changes keeping the pore water pressure, u constant. The 'bedding control' (B) maintains a constant deviator stress, $q = (\sigma_1' - \sigma_3')$ and measures the vertical displacement, where, σ_1' and σ_3' are the effective major and minor principal stresses.

There are two different modules used for undrained and drained monotonic loading where σ_3 is kept constant at the initial value. In the case of an undrained test, DPVC does not allow volume change but the change in u is measured. On the other hand, in drained test, volume change is measured while u is kept constant. The volume change and vertical displacement are used to calculate each subsequent area correction during the isotropic consolidation, monotonic loading stages and other test modules in the following two sections.

2.3.4 K_0-Consolidation Module

In the K_0-consolidation module, axial strain (ε_a) was applied at a constant rate to achieve a target vertical effective stress, σ_1'. During this vertical straining, zero radial strain was enforced by the DPVC in the manner described by Menzies (1988). At a user selected time step the computer program calculates a volume, Δv equal to the axial deformation increment times the current cross-sectional area of the specimen. The program then commands the DPVC to extract the volume Δv to maintain zero radial strain according to the following equation:

$$\varepsilon_v = \varepsilon_a + 2\varepsilon_r \rightarrow \quad \varepsilon_r = 0 = \frac{(\varepsilon_v - \varepsilon_a)}{2} \quad \rightarrow \quad \varepsilon_a = \varepsilon_v \tag{1}$$

where, $\varepsilon_a, \varepsilon_r, \varepsilon_v$ are the axial strain, radial strain and volumetric strains, respectively. The extraction of pore fluid acts to reduce the pore water pressure, but this is maintained constant by increasing the cell pressure as $\Delta u = B\Delta\sigma_3$. The volume and cell pressure are controlled by the DPVC and pressure regulator, respectively at small intervals (default 6 sec) to maintain both zero radial strain and constant pore water pressure.

A process of lowering the pore pressure was used by Uchida et al. (2003) in maintaining the K_0-condition, while using initially higher stress levels, starting with a back pressure of nearly 1500 kPa. However, the reduction of the relatively small back pressures of (400 kPa used in this study) during K_0-consolidation may risk partial de-saturation of the specimen. Therefore, cell pressure was increased in this module to keep pore pressure constant.

Once the consolidation path is completed, the program has two exit modes; either 'freeze stress' or 'freeze strain'. In the 'freeze stress' mode the control program keeps cell pressure, deviator stress and back pressure at their final values. Granting that pore pressures may still be equalizing to some degree, and that the specimen may creep a small amount, the final K_0 condition may be compromised if the specimen is held in this state for a protracted length of time. On the other hand, in the 'freeze strain' mode, the ram is stopped at the exit of K_0-consolidation i.e., axial strain is fixed, and the DPVC ceases volume change and reverts to pore pressure measurement. Cell pressure and pore pressure remain constant, but the deviator stress may keep changing slightly depending on specimen stiffness.

2.3.5 Stress Path Testing Module ($p - q - u$ table)

This module produces a sequence of stress path segments defined by the successive lines in a table called $p - q - u$ table. The appropriate testing conditions and target values to perform a desired stress path test to read from an ASCII text file. Table 2 provides an example of the testing parameters to define the stress path for one CSD and one CMS tests as performed in this study. The headings, q, p and u in Table 2 are deviator stress, mean stress $(\sigma_1 + 2\sigma_3)/3$ and pore water pressure, respectively, where σ_1 and σ_3 are the major and minor principal stresses, respectively. Ram movement control state can be either strain control (S) or bedding control (B). In strain control (S) mode, constant strain rate is applied and the rate of change to q depends on the specimen stiffness. In this case, cell pressure is constant, and the value of p is ignored by the control program. A test segment will end as soon as any of the limiting values of q, duration or strain limit is reached. In bedding control (B) mode, rate of change of q and p depends on the input stage duration. The value of strain rate is ignored by the control program. Any segment will end as soon as either q, p or strain limit is reached. DPVC state can be any of the three states; undrained (U), drained (D) and K_0-consolidation (K) state. In undrained (U) state DPVC measures the pore water pressure, u and the input value of u in $p - q - u$ table is ignored. In drained (D) state DPVC measures the volume change of the specimen and target u at the end of test is inputted. The rate of change of u is determined using the stage duration. The K_0-consolidation (K) state of DPVC if used in Table 2 is similar to that stated in previous section 2.3.4 except a pore water pressure is allowed to change.

Table 2 Control data entry in $p-q-u$ table

Test	Ram state	q	p	DPVC state	U	Strain rate	Duration	Strain limit
		kPa	kPa		kPa	%/min.	min.	%
CSD04	S	100	0.99	D	400	0.02	500	35
	B	100	400	D	400	0.99	467	35
CMS04	S	100	0.99	D	400	0.02	500	35
	B	600	633.3	D	400	0.99	334	35

3. MATERIALS AND TESTING PROGRAM

3.1 Materials

Yellow sand (YS) from Mount Compass of South Australia is tested in this study. The sand is poorly graded, uniform, sub-rounded in shape containing 10% fines, classified as SP-SM according to the Unified Soil Classification System (USCS). The coefficient of uniformity (C_u) and co-efficient of curvature (C_c) were 3.16 and 1.23, respectively. The maximum and minimum void ratios are 0.423 (1.86 g/cm3) and 0.892 (1.40 g/cm3) according to ASTM D-4253 (2004) and ASTM D-698 methods, respectively.

3.2 Specimen Preparation and Testing Method

Laboratory reconstituted specimens were prepared in this study using moist tamping method as this method reduces segregation of fines from sand (Baki et al., 2012; Rahman, 2009) and relatively loose specimens can be prepared with high void ratio. A split mould was placed over the bottom platen of the triaxial cell and then a cylindrical rubber membrane was held inside the mould using a small vacuum (-10 kPa). Oven dried natural silty sand mixed with 5% (by mass) water and cured for 24 hrs before moist tamped in equal ten layers in a split mould of 100 mm in diameter and 100 mm in height. The specimen was compacted in 10 layers to increase the homogeneity and reduce the variation in local density between layers. The thickness of each layer was controlled using a height controlled tamping rod as shown in Figure 3.

(a) (b)

Figure 3 Height controlled tamping rod: (a) components of tamping rod and (b) tamping rod in use

In this study, the end friction was removed by using lubricated free ends and enlarged end platens as introduced by Lo et al. (1989). The 20% larger end platens (120 mm diameter) provide enough space for lateral expansion of soil specimen undergoing large axial strain. The free ends are achieved by placing a latex membrane of diameter slightly bigger than the specimen diameter placed over the enlarged platen lubricated with a thin film of high vacuum grease. The latex membranes were pre-stressed to a maximum stress likely during testing to obtain a uniformly greased film. Uniform grease thickness is important to ensure uniform contact between soil sample and uniform deformation at high axial strain (Bobei et al., 2009; Lo et al., 2010). A small circular opening was made at the middle of the latex membrane with a diameter equal to the porous stone (35 mm) so that water movement was not hindered by the latex membrane. The thickness of the rubber membrane used in developing free ends was 0.50 mm to prevent the larger sand particles penetrating the membrane and coming in contact with the platen. The effectiveness of free end and enlarged end platens can be shown in Figure 4 at large axial strain of 35%.

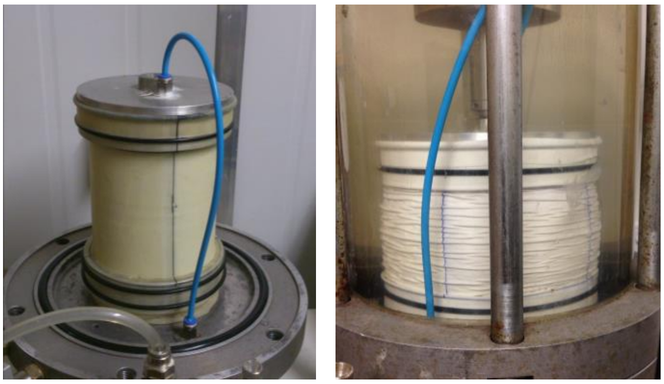

(a) (b)

Figure 4 Effectiveness of lubricated free end: (a) specimen after preparation and (b) uniform deformation after 35% axial strain

Once the specimen preparation was finished, CO_2 percolation and back pressure saturation were performed to achieve a Skempton's B value of 0.98 or higher. The back pressure module was used to apply cell pressure and back pressure at increments of 2 kPa/min. up to 420 kPa and 400 kPa, respectively. After that the specimen was consolidated to a desired mean effective stress, p_0', for the isotropic condition, or to an effective vertical stress, σ_{v0}', for the K_0 condition where '0' refers the end of consolidation or commencement of shearing. Then specimens were sheared according to the desired stress path i.e., undrained, drained, CSD or CMS. In case of CSD and CMS tests, specimens were first sheared under conventional drained path up to a pre-defined deviator stress, q or stress ratio, $\eta = q/p'$ before commencing the CSD or CMS path. CSD path was achieved by gradually reducing σ_3, keeping q and u constant. On the other hand, CMS path can be obtained by reducing σ_3 in a controlled way so that mean effective stress, p' and u keep constant. Typical stress paths for all the tests are shown in Figure 5.

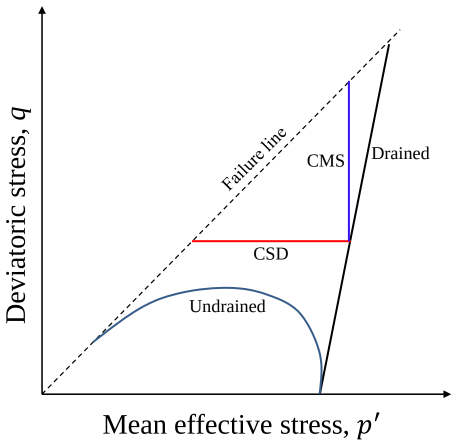

Figure 5 Typical stress path

4. EXPERIMENTAL RESULTS

4.1 Undrained Tests after Isotropic and K_0-Consolidation

Undrained triaxial compression tests were performed after the specimens were consolidated isotropically and K_0-condition. Isotropic consolidation module was used in case of isotropic consolidation where σ_3 was raised at a constant rate keeping u constant. K_0-consolidation module was used for K_0-consolidation where a constant vertical strain rate of 0.015% per min. was applied to achieve a target effective vertical stress σ_1'. A small vertical strain rate was applied to limit the development of pore water pressure during the consolidation phase. Negligible ε_r and u changes were achieved during the K0-consolidation phase for all the tests as in Figure 6 for YS-K0U08 as an example. Zero radial strain was calculated using the measured data ε_a and ε_v from the ram displacement and DPVC, respectively.

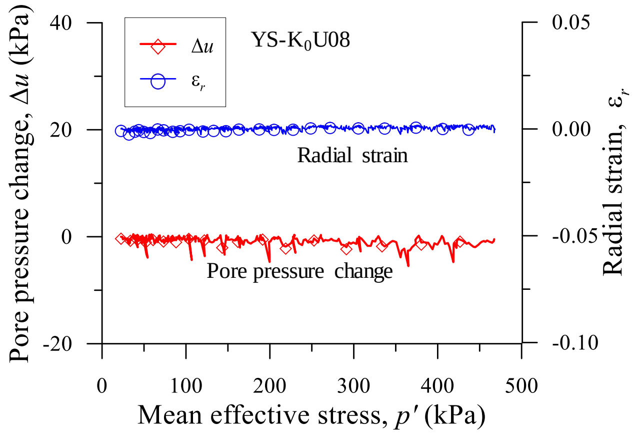

Figure 6 Zero radial strain and pore pressure during K0-consolidation

K0-consolidation started from a reference isotropic stress state $\sigma_1' = \sigma_3' \approx 20$ kPa, i.e., K ≈ 1. Initially, K decreased sharply with increasing p' before reaching an almost steady value of K0 at higher p' as shown in Figure 7 for test YS-K0U08 and YS- K0U13. This is observed for all the tests in this study and consistent with earlier K0 studies under triaxial testing system (Lo and Chu, 1991), thin wall oedometer (Lee et al., 2013) and DEM simulation (Nguyen et al., 2014). It can be observed that the K0 value travels towards a constant value despite the initial drift of some curves (between 20 to 30 kPa) due to the initial seating problem of the loading ram.

K0-consolidaion test results are compared with oedometer test results of the same sand (YS) performed for other studies (Rabbi et al., 2014; Rabbi et al., 2014), in $e - \log(\sigma_1')$ space as shown in Figure 8. Vertical effective stress, σ_1' instead of mean stress is used for comparison basis due to the limitation in measurement of lateral stress in oedometer tests. Three oedometer tests shown were performed on saturated specimens prepared at different initial void ratio, e_i and incrementally loaded from 12.5 kPa to 800 kPa. K0-consolidated tests were selected so that e_i covers a range of values. It can be observed that there is good agreement of the slope of the curves from K0-consolidation to the oedometer tests which is a good indication of controlling of the K0-condition and the accuracy of the measurement system of the new triaxial device. Therefore, K0-consolidation tests in this system can be used as an alternative to oedometer tests, along with the measurement of radial stress development, i.e., K0.

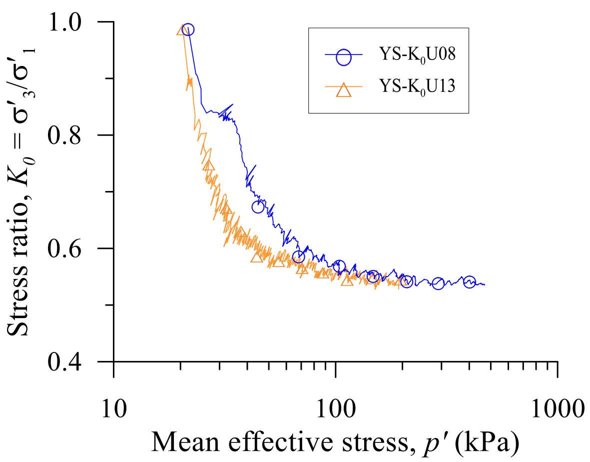

Figure 7 Variation of K0 = σ_3'/σ_1' with mean effective stress

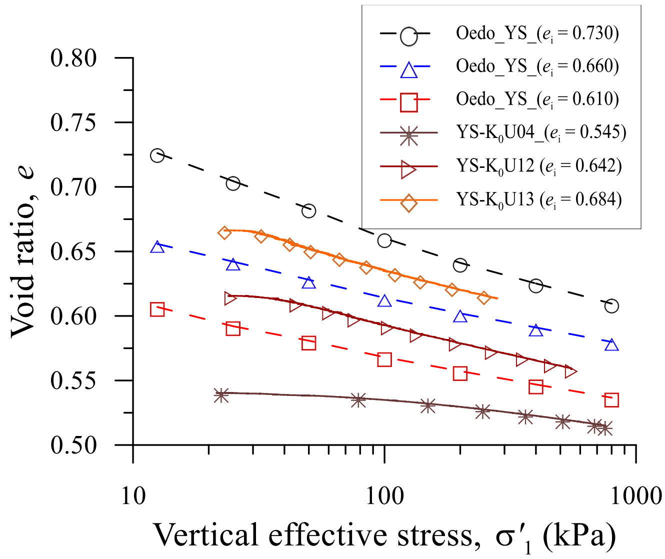

Figure 8 Comparison of K0-consolidation test with oedometer tests

Figure 9 shows the test result obtained from one CIU (YS-CIU07) and K0U (YS-K0U07). YS-CIU07 is isotropically consolidated to an initial mean effective stress, p_0' of 350 kPa before undrained shearing. For specimen YS-K0U07, σ_1' = 400 kPa was targeted during the K0-consolidation phase before starting the undrained shearing. The void ratios after consolidation of the specimens are different due to the higher axial strain during K0-consolidation ($\varepsilon_a \approx 1.8\%$) than isotropic consolidation ($\varepsilon_a \approx 0.7\%$). Figure 9(a) shows the stress-strain behaviour of the isotropically consolidated and K0-consolidated specimens. For both the tests deviator stress, q increases initially with axial strain, ε_a and then drops down to a critical state condition of d$q \approx 0$. However, the peak deviator stress developed very quickly for K0 specimen after starting the undrained shearing at $\varepsilon_a \approx 0.3\%$ compared to isotropic specimen at $\varepsilon_a \approx 2.1\%$. Figure 9(b) shows the effective stress path (ESP) of the isotropic and K0-consolidated specimens. The ESP of YS-K0U07 for the K0 phase is also shown in the graph which started at point O and finished at point A where the values of q, σ_3' and p_0' developed 186, 215 and 278 kPa, respectively. The K0 value obtained for this test is 0.538 and ranges between 0.48 and 0.55 for all the tests. Once the shearing starts the specimen shows a clear peak q and drops down to follow the failure envelope. Both the tests follow the similar path to the failure envelope after the initial peak. Figure 9(c) shows the pore water pressure, u development with ε_a for both the tests. Both tests developed u sharply at small axial strain and then reached a critical state condition du = 0 at large axial strain. Therefore, critical state can be reached in the newly developed system with homogeneous stress-strain distribution (Figure 4).

4.2 Drained Tests after Isotropic and K0-Consolidation

Similar to undrained tests, results from drained triaxial compression tests were presented in Figure 10 for isotropic and K0-consolidated specimens. YS-CID01 is isotropically consolidated to p_0' of 50 kPa before starting the drained shearing while a target σ_1' = 100 kPa was directed for specimen YS-K0D03 during the K0-consolidation phase before starting the undrained shearing. After the K0-consolidation, YS-K0D03 achieved values of q, σ_3' and p_0' are 42, 55 and 72 kPa, respectively. The deviator stress, q for both specimens (YS-CID01 and YS-K0D03) increased gradually with increasing axial strain, ε_a. Critical state condition i.e., d$q \approx 0$ and d$\varepsilon_v \approx 0$, was reached at large axial strain without showing any clear peak which is typical for loose specimens as shown in Figure 10. The volume change behaviour shows that both the specimens compressed with increasing ε_a and reached a condition of negligible volume change with continuous increase in ε_a, i.e., critical state condition. This type of behaviour is referred to as contractive behaviour.

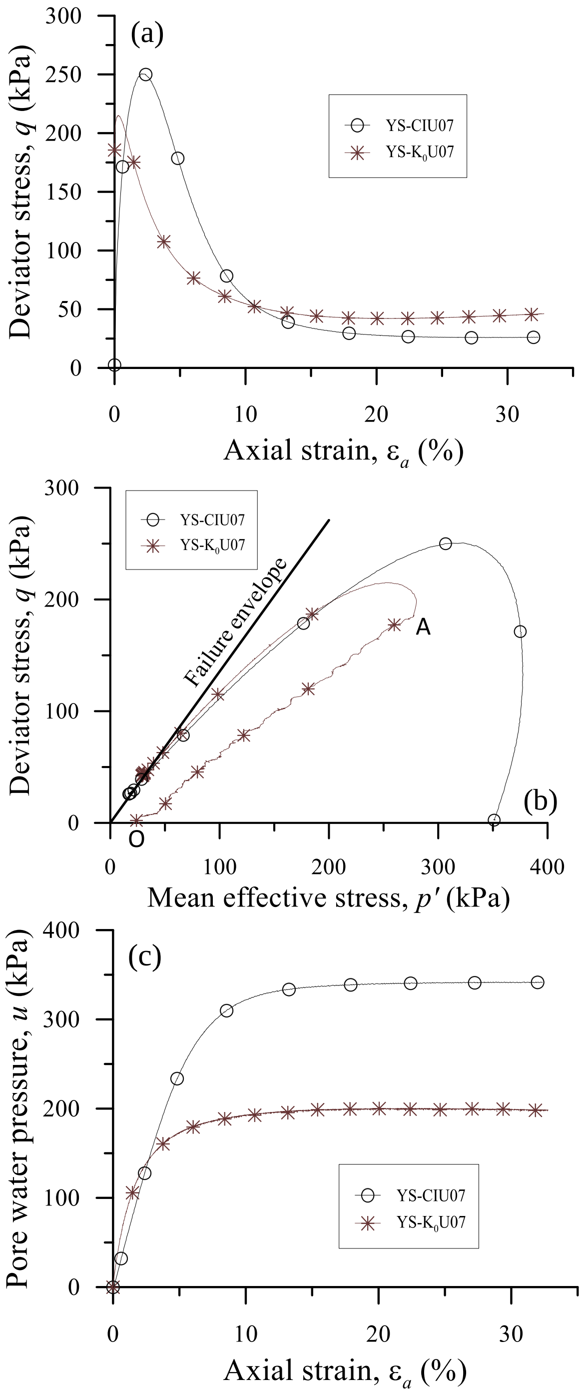

Figure 9 Undrained behaviour of sand after isotropic and K_0-consolidation: (a) stress-strain (b) effective stress path, and (c) pore water pressure development

4.3 Constant Shear Drained (CSD) Tests

CSD tests performed after specimens were isotropically consolidated to a desired p'_0. Specimens were first sheared under conventional drained path up to a pre-defined q before commencing the CSD path. $p-q-u$ table was used to define both a conventional drained path and CSD path as presented for test CSD04 in Table 2. The first line in the $p-q-u$ table was used to define a conventional drained path under strain control (S) mode where, the ram moved at a constant strain rate of 0.02 %/min. to achieve a target q of 100 kPa (the value of p is ignored). Pore water pressure, u was kept constant at 400 kPa under a drained (D) DPVC state. This path ended as soon as either of the target q = 100 kPa, duration = 500 min. or strain limit = 35% was reached. Once the conventional drained path finished the control starts the next path immediately, namely a CSD path under bedding control (B) mode in this case. CSD stress path is maintained by keeping q = 100 kPa and reducing p from 633 kPa (value at the end of conventional drained path) to 400 kPa at duration of 467 min. The bedding control (B) mode reached the target p by reducing σ_3 at a rate of 0.5 kPa/min.; the rate depends on the difference in p and duration. The stress path ended as soon as either of the target p = 400 kPa, duration = 467 min. or strain limit = 35% was reached. DPVC state of the CSD stress path was drained (D) so that volume change occurred to keep u constant to 400 kPa. Figure 11 shows negligible u development throughout the test CSD04 where point A represents the commencement of the CSD segment.

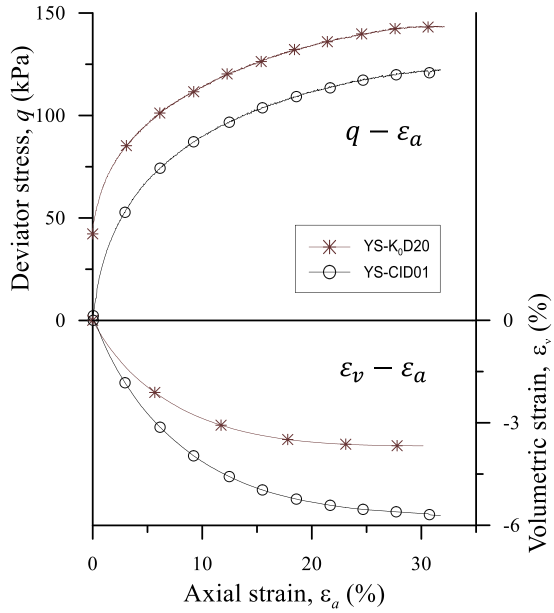

Figure 10 Drained stress-strain and volume change behaviour of sand after isotropic and K_0-consolidation

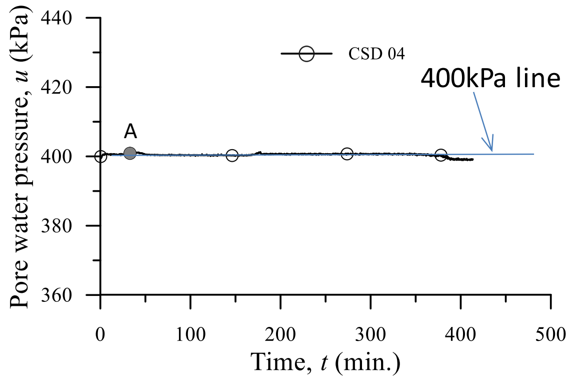

Figure 11 Pore water pressure development during CSD test

Figure 12 presents the results for the test CSD04. The commencement of CSD path is represented by point A. Effective stress path (ESP) shows that as the mean effective stress, p' decreased at the beginning of the CSD segment, q maintained a constant value up to a certain point. After that CSD stress path was unable to hold q and ESP dropped down towards the failure envelope as observed in Figure 12(a). Similar behaviour was also observed by Monkul et al. (2011) and Chu et al. (2012) for sandy soils tested under a CSD path. As soon as the ESP meets the failure envelop, it follows the failure envelope towards the origin of the $q-p'$ space which is similar to that observed by Chu et al. (2015). The volumetric strain ε_v relationship with p' shows that specimen displays contractive behaviour during the conventional drained path before commencing the CSD path. Once the CSD path started, the specimen showed slight dilative behaviour as p' reduced up to a certain point and then started rapid contractive behaviour again with further reduction in p'. There is another notable transformation of contractive to dilative behaviour of the specimen occurred at a point close to when the ESP reached failure envelope. This type of phase transformation was also observed by Monkul et al. (2011) for CSD tests and defined as characteristic state.

Figure 12(b) shows the change in confining stress, σ_3 and axial strain, ε_a over time for test CSD04. It can be observed that $p-q-u$ table was able to reduce σ_3 i.e., p at a constant rate during CSD path. Axial strain, ε_a developed slowly at the initial stage of the CSD path and then the specimen started to yield resulted a rapid development of ε_a which started at around 250 min.

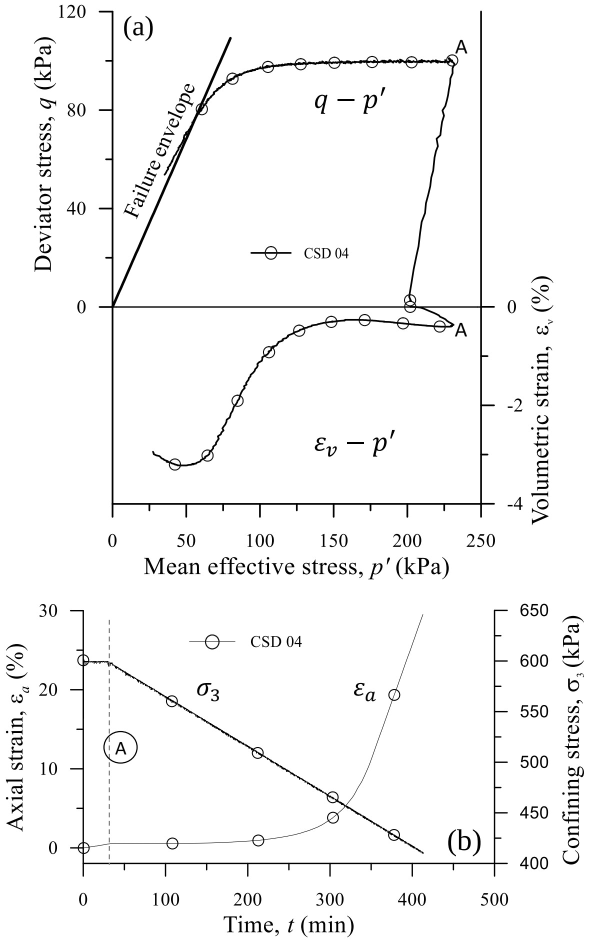

Figure 12 Constant shear drained (CSD) tests results: (a) effective stress path and volume change and (b) axial strain and confining pressure variation with time

4.4 Constant Mean Stress (CMS) Tests

Similar to CSD tests, CMS stress path tests were performed on isotropically consolidated specimens following conventional drained shearing up to a pre-defined deviator stress, q. The $p-q-u$ Table was used to define both conventional drained path and CMS path as presented for test CMS04 in Table 2. The first line in the $p-q-u$ table was the same as that used for CSD04 to achieve a q of 100 kPa in strain control (S) mode. After the conventional drained path the control starts the CMS segment as defined in the second line in Table 2. CMS stress path is maintained in bedding control (B) to target an arbitrary q = 600 kPa (generally a value greater than the strength of the soil) by keeping the value of p constant at 633 kPa (value at the end of conventional drained path). The DPVC state was drained (D); allowed volume change and kept u constant to 400 kPa. Similar to CSD path, negligible pore water pressure was developed during the CMS path. In a conventional drained path the value of p would be 800 kPa if the soil would reach the target of q = 600 kPa. To achieve a CMS path σ_3 needed to reduce in such a way that the value of p remains constant throughout the path. Duration of the CMS path was inputted 334 min. to allow reduce p from 800 to 633 kPa so that initial reduction rate of σ_3 is 0.5 kPa/min. The stress path ended as soon as either of the target q = 600 kPa, duration = 334 min. or strain limit = 35% was reached.

Figure 13 presents the results for the test CMS04. The commencement of the CMS segment is represented by point A (solid filled symbols). The shape of the stress-strain and volumetric strain curves (Figure 13(a)) are like that obtained in a conventional drained path test. Deviator stress increased initially sharply with increase in ε_a, and then reached an asymptotic value (d$q \approx 0$) at large axial strain. There is no significant difference was observed in $q-\varepsilon_a$ plot as the stress path changes from conventional drained to CMS path. Volumetric stain, ε_v showed compressive behavior; large volume decrease was observed initially and then it reached a constant volume state (d$\varepsilon_v \approx 0$) at large axial strain which fulfills the critical state condition. The effective stress path (ESP) in Figure 13(b) shows that the mean effective stress, p' remained constant after the CMS path commenced at point A with increasing q. The ESP reached the failure envelope obtained from conventional drained and undrained tests and remained there at constant q and p'. This confirms that the program is able to achieve the constant mean stress condition with adequate accuracy. It can be noted that unlike CSD tests, σ_3 changed at a variable rate over time to maintain the constant p' state as the CMS test progressed as shown in Figure 13(c). Initially σ_3 decreased at a relatively higher rate as q increased sharply at smaller ε_a. At some point when the rate of increase of q decreased and yielding started with rapid generation of ε_a, the rate of reduction of σ_3 also decreased to maintain constant $p' = q/3 + \sigma_3'$. This means the program maintains target mean stress, p by acquiring data for q and reducing σ_3 accordingly using a feedback loop. Therefore, $p-q-u$ table can perform CMS tests successfully and have potential for using other defined stress path in between CSD and CMS tests.

5. CONCLUSIONS

A computer controlled triaxial testing device is designed and commissioned in the laboratory to perform triaxial tests with automatically control and sufficiently accurate measurement facilities required to obtain critical state of soil. The unique control program has seven different modules to perform different stages of the conventional drained and undrained triaxial tests and other stress path tests such as CSD and CMS tests. The following conclusions can be drawn from the data and evidence provided in the paper:

1. The newly commissioned triaxial system is satisfactorily performing conventional drained and undrained tests as well as other stress path tests.
2. Uniform stress-strain distribution of soil specimen at large axial strain can be obtained by the specimen preparation technique and lubricated end platens used in this study.
3. K_0 condition is achieved in triaxial condition and K_0 value ranged between 0.48 and 0.55 for YS sand. The slope of K_0-consolidation in $e-log(\sigma_1')$ space matched well with the laboratory oedometer test data for YS sand.
4. Critical state condition (d$q \approx 0$, d$\varepsilon_a \approx 0$ and d$\varepsilon_v \approx 0$) at large axial strain can be achieved for conventional drained, undrained and CMS tests using the new triaxial testing device. However, critical state condition is not achieved during the CSD tests due to the inability of soil to maintain constant deviator stress (dq ≈ 0) due to continuous reduction in confining stress.
5. Volumetric strain during CSD test shows multiple changeover from dilation to compression at the start of yielding and compression to dilation near the failure state. This behaviour of sand under CSD path is also found in the literature.
6. The apparatus can control the reduction in σ_3 in a feed forward loop to maintain constant p' during a CMS test. However, the stress-strain and volume change behaviour is similar to that obtained during conventional drained path.

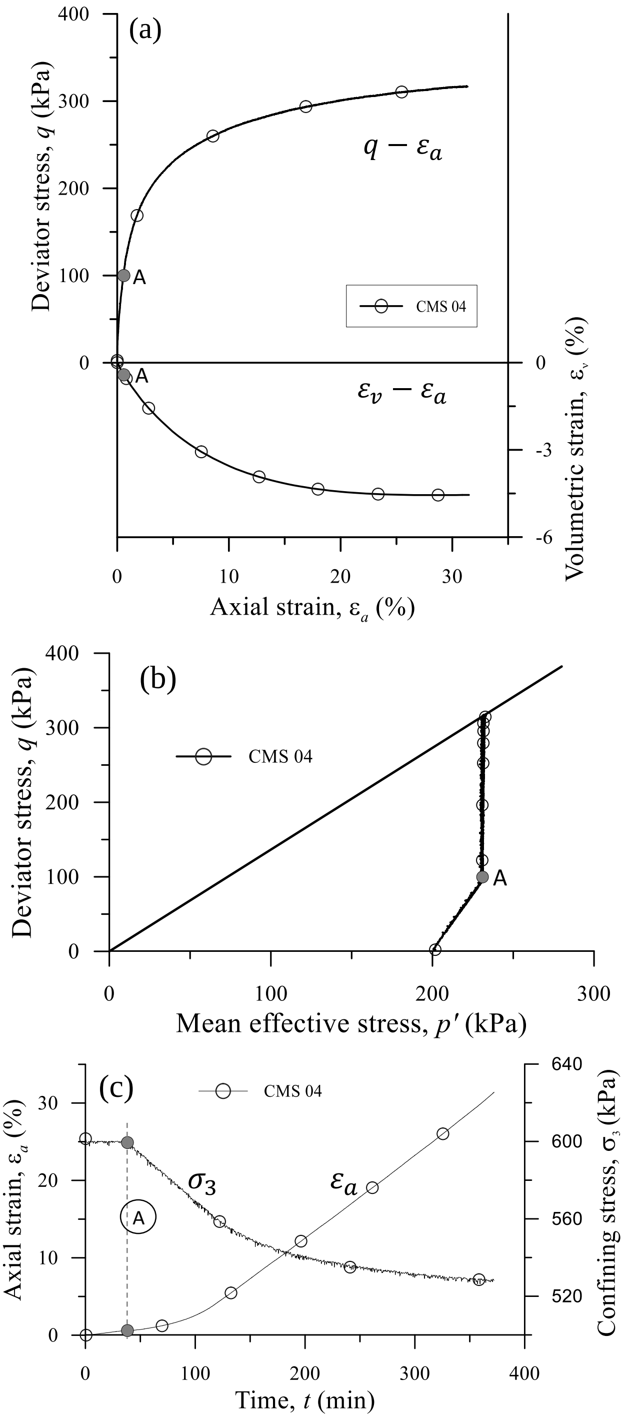

Figure 13 Constant Mean Stress (CMS) tests results: (a) deviator stress and volumetric strain change against axial strain (b) effective stress, and (c) axial strain and confining pressure variation with time

6. REFERENCES

ASTM (2004) "Standard test methods for maximum index density and unit weight of soils using a vibratory table", D 4253 - 00, ASTM International, West Conshohocken, PA 19428-2959, United States.

Baki, M. A. L., Rahman, M. M., Lo, S. R., and Gnanendran, C. T. (2012) "Linkage between static and cyclic liquefaction of loose sand with a range of fines contents" Can Geotech J, 49(8), pp891-906.

Bobei, D. C., Lo, S. R., Wanatowski, D., Gnanendran, C. T., and Rahman, M. M. (2009) "A modified state parameter for characterizing static liquefaction of sand with fines", Can Geotech J, 46(3), pp281-295.

Chu, J., Leong, W. K., Loke, W. L., and Wanatowski, D. (2012) "Instability of Loose Sand under Drained Conditions", Journal of Geotechnical and Geoenvironmental Engineering, 138(2), pp207-216.

Chu, J., Wanatowski, D., Leong, W. K., Loke, W. L., and He, J. (2015) "Instability of dilative sand", Geotechnical Research, 14.00015.

Cubrinovski, M., and Ishihara, K. (1998) "Modelling of sand behaviour based on state concept", Soils Found, 38(3), pp115-127.

Finno, R. J., and Rechenmacher, A. L. (2003) "Effects of consolidation history on critical state of sand", Journal of Geotechnical and Geoenvironmental Engineering, 129(4), pp350-360.

Fourie, A. B., and Tshabalala, L. (2005) "Initiation of static liquefaction and the role of k_0 consolidation", Can Geotech J, 42, pp892-906.

Gajo, A., Piffer, L., and De Polo, F. (2000) "Analysis of certain factors a!ecting the unstable behaviour of saturated loose sand", Mech Cohes-Frict Mat, 5, pp215-237.

GDS (2000) "ADVDPC Handbook", GDS International Limited, Hampshire, RG27 9GR U.K.

Ishihara, K. (1993) "Liquefaction and flow failure during earthquakes", Geotechnique, 43(3), pp351-415.

Jakobsen, K. P., Praastrup, U., and Ibsen, L. B. (1999) "The influence of stress path on the characteristic stress state", Proc., 2nd Int. Symposium on Pre-failure Deformation Characteristic of Geomaterials, IS Torino 99, AAU Geotechnical Engineering Group, pp659-666.

Lade, P. V., and Ibsen, L. B. (1997) "A study of the phase transformation and characteristic lines of sand", Proc., Deformation and progressive failure in geomechanics, pp353-358.

Lee, J., Yun, T. S., Lee, D., and Lee, J. (2013) "Assessment of Ko correlation to strength for granular materials", Soils Found, 53(4), pp584-595.

Lo, S. C. R., and Chu, J. (1991) "The measurement of Ko by triaxial strain path testing", Soils Found, 31(2), pp181-187.

Lo, S. R., Chu, J., and Lee, I. K. (1989) "A technique for reducing membrane penetration and bedding errors", Geotech Test J, 12(4), pp311-316.

Lo, S. R., Rahman, M. M., and Bobei, D. C. (2010) "Limited flow behaviour of sand with fines under monotonic and cyclic loading", Geomechanics and Geoengineering, 5(1), pp15-25.

Menzies, B. K. (1988) "A computer controlled hydraulic triaxial testing system", Advanced Triaxial Testing of Soil and Rock, R. T. Donaghe, R. C. Chaney, and M. L. Silver, eds., ASTM, Philadelphia, pp82-94.

Monkul, M. M., Yamamuro, J. A., and Lade, P. V. (2011) "Failure, instability, and the second work increment in loose silty sand", Can Geotech J, 48(6), pp943-955.

Murthy, T. G., Loukidis, D., Carraro, J. A. H., Prezzi, M., and Salgado, R. (2007) "Undrained Monotonic Response of Clean and Silty Sands", Geotechnique, 57(3), pp273-288.

Nguyen, H. B. K., Rahman, M. M., Cameron, D. A., and Fourie, A. B. "The effect of consolidation path on undrained behaviour of sand - A DEM approach", Proc., 14th Int. Conference of International Association for Computer Methods and Recent Advances in Geomechanics, IACMAG 2014, pp175-180.

Nguyen, H. B. K., Rahman, M. M., and Fourie, A. B. (2016) "Undrained behaviour of granular material and the role of fabric in isotropic and K0-consolidation: DEM approach", Geotechnique.

Omar, T., and Sadrekarimi, A. (2014) "Effect of multiple corrections on triaxial compression testing of sands", Journal of GeoEngineering, 9(2), 75-83.

Rabbi, A. T. M. Z., Donald, A. C., and Rahman, M. M. (2014) "Effect of initial partial saturation on collapse behavior of glacial sand with fines", GeoCongress 2014, Geo-Institute, ASCE, Atlanta, USA, pp103-112.

Rabbi, A. T. M. Z., Rahman, M. M., and Cameron, D. A. (2014) "Prediction of collapse potential for silty glacial sand", Australian geomechanics, 49(3), pp65-77.

Rabbi, A. T. M. Z., Rahman, M. M., and Cameron, D. A. (2018) "Undrained Behavior of Silty Sand and the Role of Isotropic and K0 Consolidation", Journal of Geotechnical and Geoenvironmental Engineering, 144(4), 04018014.

Rabbi, A. T. M. Z., Rahman, M. M., and Cameron, D. A. (2019) "Critical State Study of Natural Silty Sand Instability under Undrained and Constant Shear Drained Path", International journal for geomechanics, 19(8), 04019083.

Rabbi, A. T. M. Z., Rahman, M. M., and Cameron, D. A. (2019) "The relation between the state indices and the characteristic features of undrained behaviour of silty sand", Soils and Foundation, 59(4), 801-813.

Rabbi, A. T. M. Z., Rahman, M. M., and Donald, A. C. (2014) "Undrained behaviour of silty glacial sand", GeoCongress 2014, Geo-Institute, ASCE, Atlanta, USA, pp139-148.

Rahman, M. M. (2009) "Modelling the influence of fines on liquefaction behaviour", PhD Thesis, University of New South Wales at Australian Defence Force Academy, Canberra, Australia.

Rahman, M. M., and Lo, S. R. (2012) "Predicting the onset of static liquefaction of loose sand with fines", Journal of Geotechnical & Geoenvironmental Engineering, 138(8), pp1037-1041.

Rahman, M. M., and Lo, S. R. (2014) "Undrained behaviour of sand-fines mixtures and their state parameters", Journal of Geotechnical and Geoenvironmental Engineering, 140(7), 04014036.

Rahman, M. M., Lo, S. R., and Gnanendran, C. T. (2008) "On equivalent granular void ratio and steady state behaviour of loose sand with fines", Can Geotech J, 45(10), 1439-1455.

Roscoe, K. H., Schofield, M. A., and Worth, C. P. (1958) "On the yielding of soils", Geotechnique, 8(1), pp22-53.

Rowe, P. W., and Barden, L. (1964) "Importance of free ends in triaxial testing", Journal of Soil Mechanics and Foundation Division, ASCE, 90(1), pp1-15.

Sasitharan, S., Robertson, P. K., Sego, D. C., and Morgenstern, N. R. (1993) "Collapse behaviour of sand", Can Geotech J, 30(4), pp569-577.

Schofield, A., and Worth, P. (1968) Critical State Soil Mechanics, McGraw-Hill, London.

Thevanayagam, S., Shenthan, T., Mohan, S., and Liang, J. (2002) "Undrained fragility of clean sands, silty sands, and sandy silts", Journal of Geotechnical and Geoenvironmental Engineering, 128(10), pp849-859.

Uchida, K., Stedman, D. J., and Sakagami, T. (2003) "Strain-path Control Ko Consolidation of Marine Clays", Proc., Thirteenth International Offshore and Polar Engineering Conference, The International Society of Offshore and Polar Engineers, 555-560.

Yang, J. (2002) "Non-uniqueness of flow liquefaction line for loose sand", Geotechnique, 52(10), pp757-760.

Zhang, J., Lo, S.-C. R., Rahman, M. M., and Yan, J. (2017) "Characterizing Monotonic Behaviour of Pond Ash within Critical State Approach", Journal of Geotechnical and Geoenvironmental Engineering.

Zhu, J. H., and Anderson, S. A. (1998) "Determination of shear strength of Hawaiian residual soil subjected to rainfall-induced landslides", Geotechnique, 48(1), pp73-82.